Functional characterisation of the actin-depolymerising factor from the apicomplexan Neospora caninum (NcADF)

Functional characterisation of the actin-depolymerising factor from the apicomplexan *Neospora caninum* (NcADF)

Luciana Baroni,[a] *Luiz M. Pereira,*[a] *Sutherland K. Maciver,*[b,†] *Ana P. Yatsuda*[a,†,*]

[a] Faculdade de Ciências Farmacêuticas de Ribeirão Preto, Universidade de São Paulo, Av. do Café, s/n, 14040-930, Ribeirão Preto, SP, Brazil.

[b] Centre for Discovery Brain Sciences, Biomedical Sciences, Edinburgh Medical School, University of Edinburgh, Hugh Robson Building, George Square, Edinburgh EH8 9XD, Scotland, United Kingdom.

[†]SKM and APY are co-senior authors.

Corresponding author: Departamento de Análises Clínicas, Bromatológicas e Toxicológicas, Faculdade de Ciências Farmacêuticas de Ribeirão Preto, Universidade de São Paulo, Ribeirão Preto-SP, 14040-930, Brazil. Email address: ayatsuda@fcfrp.usp.br. Tel: +55 16 33154728 (APY).

Abbreviations:

Actin-binding protein (ABP); actin-depolymerising factor (ADF); actin filaments (F-actin); actin in monomeric form (G-actin); actin conjugated to pyrene (PI-actin)

Abstract

Neospora caninum is an apicomplexan parasite that causes infectious abortion in cows. As an obligate intracellular parasite, *N. caninum* requires a host cell environment to survive and replicate. The locomotion and invasion mechanisms of apicomplexan parasites are centred on the actin-myosin system to propel the parasite forwards and into the host cell. The functions of actin, an intrinsically dynamic protein, are modulated by actin-binding proteins (ABPs). Actin-depolymerising factor (ADF) is a ubiquitous ABP responsible for accelerating actin turnover in eukaryotic cells and is one of the few known conserved ABPs from apicomplexan parasites. Apicomplexan ADFs have nonconventional properties compared with ADF/cofilins from higher eukaryotes. In the present paper, we characterised the ADF from *N. caninum* (NcADF) using computational and *in vitro* biochemical approaches to investigate its function in rabbit muscle actin dynamics. Our predicted computational tertiary structure of NcADF demonstrated a conserved structure and phylogeny with respect to other ADF/cofilins, although certain differences in filamentous actin (F-actin) binding sites were present. The activity of recombinant NcADF on heterologous actin was regulated in part by pH and the presence of inorganic phosphate. In addition, our data suggest a comparatively weak disassembly of F-actin by NcADF. Taken together, the data presented herein represent a contribution to the field towards the understanding of the role of ADF in *N. caninum* and a comparative analysis of ABPs in the phylum *Apicomplexa*.

1. Introduction

48 *Neospora caninum*, the etiological agent of neosporosis, represents one of the main causes of infectious abortion in milk and beef cattle [1]. Additionally, the infection of a herd is associated 50 with significant global economic losses to the cattle industry, estimated to be greater than one billion dollars annually [2]. Together with other significantly threatening parasites to human 52 and animal health such as *Toxoplasma gondii*, *Plasmodium*, *Cryptosporidium*, *Eimeria,* and *Theileria, N. caninum* belongs to the phylum *Apicomplexa*. These obligate intracellular 54 parasites make use of filamentous actin (F-actin) in a specific mechanism of invasion and locomotion, named gliding motility [3], to access the intracellular content of host cells. The 56 cellular machinery responsible for gliding motility is composed of specialised protein associations, including an actin-myosin motor, which generate the propulsion force that moves 58 parasites forwards [4-6]. Although apicomplexan actin may not be a determinant for host cell invasion [7, 8], it is essential for the egress of *T. gondii* from the parasitophorous vacuole [8,9] 60 and for apicoplast replication [7-9]. In addition to the use of F-actin during gliding motility, apicomplexan actin shows unusual properties, forming short and unstable filaments *in vitro* 62 [10,11], as well as highly abundant intracellular monomeric actin (G-actin) as compared with F-actin *in vivo* [5,6]. The model of polymerisation proposed for *T. gondii* actin is based on the 64 independence of the nucleation phase [12], in contrast to *P. falciparum* actin I, which depends on nucleation to polymerise [13].

66 A limited set of conserved actin-binding proteins (ABPs) is found in apicomplexan organisms [4, 14] and these proteins interact with actin and regulate its activity. ADF/cofilins 68 are ubiquitous ABPs composed of an ADF-homology domain (ADF-H), responsible for interaction with G- and F-actin [15, 16]. Proteins in this family have a role in regulating actin 70 dynamics, mainly favouring F-actin disassembly by depolymerisation and/or severing [17]. There is no consensus on the manner by which homologous and orthologous ADF/cofilins

72 cause F-actin disassembly. The extent of their effects on actin may vary across different species
[18]. Moreover, the function of yeast cofilin is known to depend on the proportion of actin and
74 cofilin [19].

ADF has been characterised in *T. gondii* [20-23] and *Plasmodium* [21, 24-26] as one and two
76 isoforms, respectively. Apicomplexan ADFs, with the exception of *P. falciparum* ADF2
(PfADF2), have a smaller F-actin binding site (F-loop) and a truncated C-terminal β-strand as
78 compared with other ADF/cofilin family members, which could partly explain its unusual
properties [20, 24, 46]. *T. gondii* ADF (TgADF), expressed in cytoplasm [20], displays a
80 primary function of monomer sequestering, with evidence of relatively weak F-actin severing
[23]. ADF1 from *Plasmodium falciparum* (PfADF1), cytoplasmic and broadly expressed in
82 parasite stages [26], has been shown to have no effect on the polymerisation of homologous or
heterologous actin [26, 27]; however, a monomer-sequestering function was detected [27]. The
84 severing activity of PfADF1 was observed in heterologous actin and later confirmed [25, 26].
PfADF1 can disassemble heterologous actin filaments; nevertheless, this ability is
86 comparatively more pronounced in TgADF [21]. The second isoform (PfADF2) is expressed
in sexual forms of *Plasmodium* [28] and is structurally more conserved than PfADF1, being
88 able therefore to bind to heterologous F-actin and sever actin filaments [24]. Here, we identified
and characterised ADF from *N. caninum* (NcADF) using computational approaches and *in vitro*
90 biochemical assays. NcADF presents a conserved tertiary structure, maintaining the main
singularities of apicomplexan ADFs. The activity of recombinant NcADF on heterologous
92 actin was determined using classical biochemistry assays, allowing an overall comparison with
homologous ADF/cofilins and insight into NcADF function.

94

96

2. Material and Methods

2.1 In silico characterisation.

Searches of genes that encode ADF in *N. caninum* genome were carried out in ToxoDB 7.3 [29] using the key-word "actin-depolymerising factor". After selection of a putative candidate, the presence of expressed isoforms was analysed using BLASTp tool in *N. caninum* database in ToxoDB. Additionally, the analysis for conserved domains were performed by Pfam 30.0 [30]. A multiple sequence alignment with homologous protein sequences was performed in MegAlign (DNASTAR, Lasergene) using Clustal W method and visualised in GeneDoc [31] employing the following sequences (UniProt sequence identification number): *Arabidopsis thaliana* ADF1 (AtADF1; Q39250), *Acanthamoeba castellanii* actophorin (P37167), *Saccharomyces cerevisiae* (ScCofilin; Q03048), *Homo sapiens* ADF1 (HsADF1; P60981), *Plasmodium falciparum* ADF1 (PfADF1; Q8I467), *P. falciparum* ADF2 (PfADF2; Q8ID92), *Eimeria tenella* ADF (EtADF; A2TEQ1), *Toxoplasma gondii* ADF (TgADF; O15902) and *N. caninun* ADF (NcADF; F0VCT8). Theoretical pI was calculated by ProtParam (https://web.expasy.org/protparam/).

2.2 Homology modelling

The tertiary structure of NcADF (ToxoDB ID NCLIV_012510/GenBank ID XP_003881486) was obtained by homology modelling using four structures as a multiple template. The following templates (with PDB ID numbers:chain) were identified after searches of NcADF on Protein Data Bank using BLASTp [30]: *A. castellanii* actophorin (1AHQ:A), *A. thaliana* ADF1 (1F7S:A), *P. falciparum* ADF1 (3Q2B:A) and *T. gondii* ADF (2L72:A). The model was built by Modeller 9.12 [32] and refined by ModRefiner [33]. The quality of model was analysed by PROCHECK [34] through PVSV 1.5 (https://psvs-1_5-dev.nesg.org), Verify3D [35] through SAVES 4 (https://services.mbi.ucla.edu/SAVES/) and Molprobity 4.3

[36]. The structures were visualised and aligned by PyMOL 1.5.0.4 (The PyMOL Molecular
122 Graphics System, Schrödinger, LCC).

2.3 *N. caninum* culture and total RNA isolation

124 Tachyzoites of *N. caninum* Nc-1 isolate were maintained in Vero cells monolayers as previously described [37]. Purified tachyzoites were obtained by exclusion chromatography
126 (Sephadex G-25, GE Healthcare). Total RNA was extracted from 7.5 x 10^7 tachyzoites using Trizol (Thermo Fisher Scientific) which was added (1 ml) to the pellet of tachyzoites and
128 incubated at room temperature for 5 minutes. Subsequently, 200 µl of chloroform were added to the tachyzoites and incubated for 3 minutes at room temperature. The tube was centrifuged
130 at 9,500 x *g* for 15 minutes at 4ºC and total RNA was precipitated from the aqueous phase using isopropanol.

132 2.4 Cloning, expression and protein purification of NcADF

The synthesis of cDNA was performed using total RNA as template by reverse transcriptase
134 (GoScript Reverse Transcription System, Promega). The cDNA was amplified by PCR using sequence-specific primers: forward (5` TTTGGATCCTCCGGAATGGGTGTT 3`; *BamH*I site
136 underlined) and reverse (5` TTTAAGCTTTGCGAGGGATGC 3`; *Hind*III site underlined). The 350 bp fragment was purified, subcloned in pGEM-T-Easy (Promega) and transformed
138 into *Escherichia coli* TOP 10 (Life Sciences). The insert sequence was verified by DNA sequencing.

140 The insert was cloned into pET28a(+). The recombinant protein NcADF_pET28 was expressed after induction with 0.2 mM IPTG in terrific broth (TB) at 22ºC during 18 hours.
142 After expression, cells were harvested and suspended in P-buffer (50 mM Tris, pH 7.0, 300 mM NaCl, 10% glycerol, 0.1% Triton X-100, 20 mM imidazole, 1 mM PMSF, 1 mM
144 benzoamidine; or cOmplete mini protease inhibitor, Roche, as protease inhibitor in replacement

of PMSF and benzoamidine). Five rounds of freeze and thaw followed by sonication (Soniprep 150, Sanyo) or only sonication (Sonifier SLPe, Branson) were used to lyse the cells. The lysate was clarified by 4,500 x *g* centrifugation for 40 minutes and the supernatant was incubated with equilibrated Ni^{+2} resin (His-Pur, Thermo Fisher Scientific) for 30 minutes. The resin was washed with P-buffer containing 40 mM imidazole and the recombinant NcADF_pET28 was eluted in P-buffer containing 250 mM imidazole. Immediately after elution, 1 mM EDTA and 1 mM DTT were added to the solution in order to avoid protein precipitation. The buffer was changed by dialysis against storage buffer (20 mM Tris, pH 7.0, 30 mM NaCl, 5% glycerol, 0.5 mM DTT, 0.5 mM NaN_3, 1 mM PMSF, 1 mM benzoamidine). The dialysed material was stored at -70ºC. The protein in solution was quantified by spectrometry (Ultrospec 2000, Pharmacia Biochem) at 280 nm using a 1-cm-path quartz cuvette and 13,980 M^{-1} cm^{-1} as extinction coefficient, calculated by ProtParam (http://web.expasy.org/protparam/). The N-terminal 6X-his tagged NcADF_pET28 recombinant protein was employed for biochemical and functional assays.

2.5 Actin preparation

Lyophilised rabbit skeletal muscle actin and N-(1-pyrene) iodoacetamide-labelled actin (PI-actin) were purchased from Cytoskeleton Inc., reconstituted (10 mg/ml) according to the manufacturer's recommendations, and stored at -70ºC. G-actin was diluted to the appropriate concentration and centrifuged at 105,000 x *g* (Optima MAX Ultracentrifuge, Beckman, rotor TLS-55) for 20 minutes at 21ºC prior to use, unless different centrifugation conditions are indicated.

2.6 Co-sedimentation

Actin was diluted in G-buffer (5 mM Tris pH 8.0, 0.2 mM $CaCl_2$, 0.2 mM ATP, 0.5 mM DTT), and the solution was incubated on ice for 1 hour and centrifuged at 53,600 x *g* for 20

minutes at 4ºC to remove aggregates. Actin polymerisation was induced for 30 minutes at 22ºC by the addition of 10X F-buffer (500 mM KCl, 20 mM $MgCl_2$, 1 mM ATP). Subsequently, 5 µM F-actin was incubated with 0–10 µM NcADF in sedimentation buffer (50 mM KCl, 2 mM $MgCl_2$, 0.2 mM ATP, buffered with either 20 mM Tris pH 8.0 or HEPES pH 6.5) for 1 hour at 22ºC. The mixtures were centrifuged for 30 minutes at 105,000 x *g*, the supernatant was removed, and the pellet was washed once with sedimentation buffer. The pellet and supernatant were mixed in appropriate volumes of 1X and 5X Laemmli buffer, respectively. The equivalent amount of pellet and supernatant were resolved by 12% SDS-PAGE and stained with Coomassie R-250. Gels were imaged using a Fujifilm Finepix S2000HD digital camera and the bands were densitometrically quantitated using ImageJ (National Institutes of Health, USA). The statistical significance among groups was determined by unpaired, equal variance, two-tailed Student's *t*-tests using GraphPad Prism 5.01 (GraphPad Software, Inc).

2.7 PI-actin polymerisation assay

Ten percent PI-actin (5 µM in a final volume of 400 µl) was incubated with 0, 1.5, 3, and 6 µM NcADF for 10 minutes prior to the addition of 1:9 (v/v) 10X ME (500 mM $MgCl_2$, 2 mM EGTA) for Ca-ATP-actin to Mg-ATP-actin conversion. The ion conversion was incubated for 5 minutes followed by polymerisation induction with 1:9 (v/v) 10X KMEI (500 mM KCl, 10 mM $MgCl_2$, 10 mM EGTA, 100 mM imidazole pH 7.0). The fluorescence was measured at room temperature for 3,000 seconds using 365 nm excitation and 407 nm emission parameters (LS 50 Perkin-Elmer Luminescence Spectrometer). The time between the addition of KMEI and the start of the fluorescence measurement was considered. With the exception of 6 µM NcADF, which was tested once, the experiments at the remaining concentrations were repeated twice with similar results.

2.8 PI-actin fluorescence decay assay

Twenty or 25% labelled PI-actin (10 μM) was polymerised in the presence of salts by the addition of 1:9 (v/v) 10X KMEI and incubation for 1 hour at 22ºC. The decrease in fluorescence was measured over time using 365 nm excitation and 407 nm emission parameters (LS 50 Perkin-Elmer Luminescence Spectrometer) following either dilution of PI-F-actin to 1 μM in the presence of 0–10 μM NcADF in KMEI or dilution of PI-F-actin to 0.1 μM in the presence of 0–0.4 μM NcADF in G-buffer. Rate constants were calculated by plotting one phase exponential decay least-squares fitting using GraphPad Prism 5.01.

2.9 Falling ball assay – low shear viscosity

The falling ball assay was performed as described previously [38]. Briefly, a final concentration of 10 μM actin and 0–10 μM NcADF were mixed prior to the addition of 1:9 (v/v) 10X KMET (500 mM KCl, 10 mM $MgCl_2$, 10 mM EGTA, 100 mM Tris pH 8.0). The solutions were drawn up into 100 μl capillaries (Pyrex 100 μl, Corning). Following incubation for 1 hour at room temperature (~22ºC), the time required for a stainless-steel ball to travel 8 cm through the capillary was recorded manually using a timer. Gelsolin was used as a severing control at 2.5 and 5 μM concentrations. Results are expressed as normalised viscosity, measured as the velocity of the falling ball, to minimise differences between actin preparations.

2.10 Steady state

Serial dilutions of PI-G-actin (10%; 0.1–5 μM) were mixed with either 0 or 10 μM NcADF in G-buffer. Actin polymerisation was immediately induced by the addition of 1:9 (v/v) 10X KMEI and incubated at 22ºC for 19 hours. Fluorescence was measured using 365 nm excitation and 407 nm emission parameters (LS 50 Perkin-Elmer Luminescence Spectrometer). The data were analysed by linear regression using GraphPad Prism 5.01, and the equilibrium

dissociation constant (Kd) was calculated using the following equation as previously described [39].

$$Kd = ([A0] - [AG])\,[G] / [AG];$$

Where, A0 = total concentration of NcADF, AG = non-polymerisable 1:1 complex of NcADF and G-actin, and [G] = critical concentration for polymerisation of actin.

The critical concentration of actin was calculated as the intersection between the fluorescence intensity measurements for G-actin and either serially diluted F-actin or NcADF mixed with F-actin, considering the basal fluorescence of G-actin [40].

2.11 Protein binding two-dimensional electrophoresis

ATP-G-actin (5 µM) was mixed with 20 µM NcADF in Mg-G-buffer containing 15% glycerol and the mixture was incubated for 15 minutes at 22ºC. The reaction was resolved by 7.5% native polyacrylamide gel electrophoresis as described [27], with modifications. The acrylamide gels contained 150 mM Tris, pH 8.8, 0.2 mM $MgCl_2$, 0.2 mM ATP, and 0.5 mM DTT. The gels were run in Tris/glycine buffer containing 25 mM Tris, 192 mM glycine, 0.2 mM $MgCl_2$, 0.2 mM ATP, and 0.5 mM DTT in a Mighty Small II SE-250 Mini-Vertical Electrophoresis System (GE Healthcare Life Sciences) at 150 V and the cooling system at 4ºC for ~3 hours. At least three wells were run: two of them containing 20 µl reaction mixture and one containing 70 µl. After protein separation, one strip was cut and subjected to western blotting; another strip was stained with Coomassie G-250, and the third strip, containing the higher volume of reaction mixture, was placed over 12.5% SDS-PAGE, as described previously [40]. The strip of native gel was covered with sealing buffer (25 mM Tris, 192 mM glycine, 1% SDS, 0.5% agarose, traces of bromophenol blue) and ran at 150 V.

2.12 Cross-linking

Seventy microliters reaction mixture containing 10 µM actin and 10 µM NcADF were incubated in interaction buffer (50 mM HEPES, pH 8.2, 50 mM NaCl, 0.1 mM EDTA, 0.2 mM

ATP) containing either 4% formaldehyde or 2 mM 1-ethyl-3-(3-
242 dimethylaminopropyl)carbodiimide (EDC) for 30 minutes at 22ºC. EDC (1 mM) was added to the reaction at time 0 and following 15 minutes of incubation, and the reaction was stopped by
244 the addition of 9 mM glycine. The reactions were mixed with 4X Laemmli buffer and visualised by SDS-PAGE stained with Coomassie G-250. The reactions containing formaldehyde were
246 also subjected to western blotting.

2.13 Western blotting

248 Western blotting was performed as previously described [37]. The SDS-PAGE gel was transferred to a PVDF membrane (Immobilon 0.45 μM, Millipore), which was subsequently
250 blocked in PBS-GT (0.8% swine gelatin, Sigma-Aldrich, 0.05% (v/v) Tween-20 in PBS). An anti-NcADF serum was used for protein detection together with a peroxidase-conjugated anti-
252 mouse IgG secondary antibody (anti-mouse IgG – whole molecule – peroxidase, antibody produced in rabbit, Sigma-Aldrich).

254 ## 3. Results

3.1 Computational analysis of NcADF

256 One homologous ADF/cofilin sequence was identified in the *N. caninum* genome following a BLAST search as ID NCLIV_012510 in ToxoDB. The gene encoding NcADF comprises a
258 sequence containing 1,335 bp with one intron. After splicing, the sequence presents 357 bp encoding a predicted protein of 118 amino acids including the stop codon. A multiple alignment
260 of ADF/cofilin protein sequences revealed that *N. caninum* ADF (NcADF) shared 89% identity and 94% similarity with *T. gondii* ADF (TgADF), followed by 62% identity and 77% similarity
262 with *E. tenella* ADF (EtADF), and only 36% identity and 58% similarity with *P. falciparum* ADF1 (PfADF1). Non-apicomplexan ADF/cofilins shared 23–31% identity with NcADF
264 (Figure 1A). The ADF homology (ADF-H, Pfam ID pf00241) domain, a globular module

present in ADF/cofilins [15, 16], was predicted to reside between residues 9 and 117 of NcADF (Figure 1A, black line). Similar to other apicomplexan ADFs, the described binding sites of G-actin to yeast cofilin were conserved in NcADF (Figure 1A). Conversely, F-actin binding sites such as R80 and the C-terminal α-4 F-actin-binding motif were missing from NcADF (Figure 1A). Four F-actin binding residues were described in PfADF1 and two of these were conserved in NcADF; D117 and K100 (Figure 1A). The tertiary structure was predicted for NcADF (Figure 1B) based on multiple templates. The structure presented favourable values in the validation analysis (Table S1) and a structural similarity to the templates (Table S2), with a lower RMSD when aligned with TgADF, as compared with the other templates used in the model prediction (Table S2). The predicted NcADF structure observed in Pymol comprised 5 β-strands and 4 α-helices, and shared similarities with the TgADF structure (Figure 1C). In contrast, when a multiple alignment was performed considering the secondary structure of NcADF, the one-turn α-4 was not shown, and an additional β-1 strand (G6-V7) was observed (Figure 1B and A, dotted rectangle). Moreover, the β-1 was not shown in the tertiary structure (Figure 1B). For analysis, the NcADF secondary structural elements observed in the multiple alignment and tertiary structure prediction were considered; therefore, NcADF comprised six β-strands and four α-helices (Figure 1A). Certain differences were observed between the NcADF and TgADF secondary structures, encompassing α-1 and β-2 to β-5, which were smaller in TgADF (Figure 1A). Major structural divergences were present in the β-2 C-terminal region (D32 in NcADF and E32 in TgADF) and A55, between α-2 and β-4 (Figure 1A and C; Figure S1). α-1 and α-3 were conserved between the three apicomplexan ADF secondary structures analysed (Figure 1A). Moreover, TgADF was missing the one turn α-4 that is present in NcADF and PfADF1 (Figure 1A and C, arrow; Figure S1). The region composing the F-loop (situated between strands β-4 and β-5) was less pronounced in NcADF and TgADF as compared with actophorin (Figure 1D).

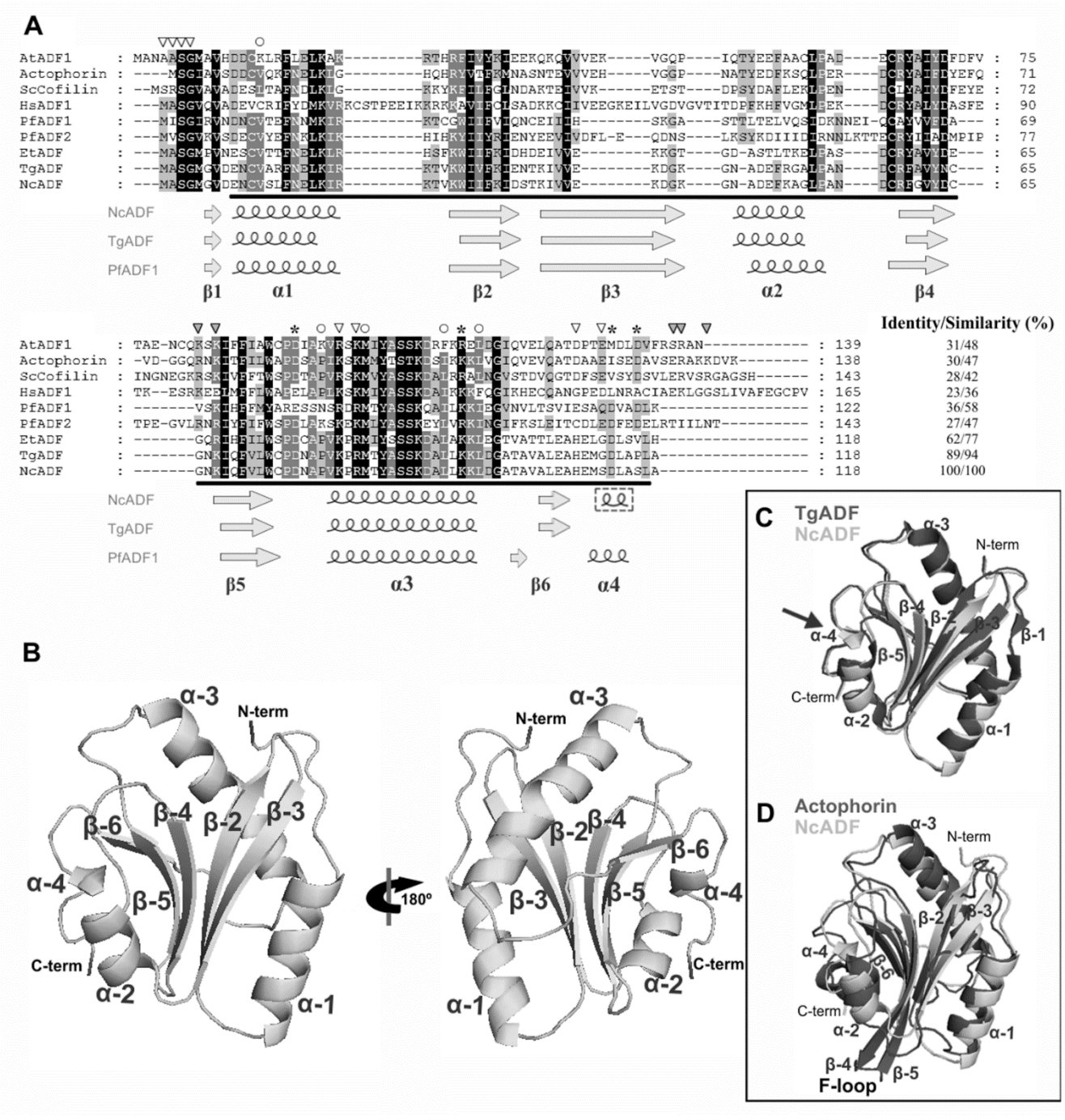

Figure 1. Multiple alignment of NcADF with representative ADF/cofilins and predicted tertiary structure of NcADF. A) Primary sequence of ADF/cofilin family members were aligned with NcADF using Clustal W algotithm. The secondary structure of *Toxoplasma gondii* ADF (TgADF), *Plasmodium falciparum* ADF1 (PfADF1) and NcADF are exposed bellow the alignment. Actin binding sites identified in yeast cofilin by site-specific mutagenesis [51] and synchrotron protein footprinting [52] are marked with tringles (Δ) and circles (○), respectively. F-actin binding sites are marked with grey tringles. In asterisks (*), the F-actin binding site 2, identified in *Plasmodium falciparum* ADF1 [25]. The ADF-H domain in NcADF is highlighted in black line. The α-4 helix, in a dotted rectangle, was observed only in Pymol and manually added to secondary structure. The sequences are: *Arabidopsis thaliana* ADF1 (AtADF1), *Acanthamoeba castellanii* actophorin (Actophorin), *Saccharomyces cerevisiae* (ScCofilin), *Homo sapiens* ADF1 (HsADF1), *P. falciparum* ADF1 (PfADF1), *P. falciparum* ADF2

(PfADF2), *Eimeria tenella* ADF (EtADF), *T. gondii* ADF (TgADF) and *Neospora caninun*
304 ADF (NcADF). **B)** Tertiary structure of NcADF obtained by homology modelling. **C)** Struc-
tural alignment of NcADF and TgADF (2L72). On the arrow, α-4 is present only in NcADF.
306 **D)** Structural alignment of NcADF and actophorin (PDB ID 1AHQ).

3.2 Recombinant NcADF expression

308 The tachyzoite-derived cDNA encoding NcADF was amplified, cloned into a pET expression plasmid, and the recombinant protein with an N-terminal 6X his-tag was expressed
310 in *E. coli* BL21(DE3). The pET28 plasmid was used for the expression of soluble NcADF, which was purified by affinity chromatography using nondenaturing buffer (Figure 2A). The
312 anti-NcADF serum (1:15,000, generated from denatured NcADF_pET32; Figure S2) was able to detect the recombinant NcADF_pET28 (in the native form) (Figure 2B).

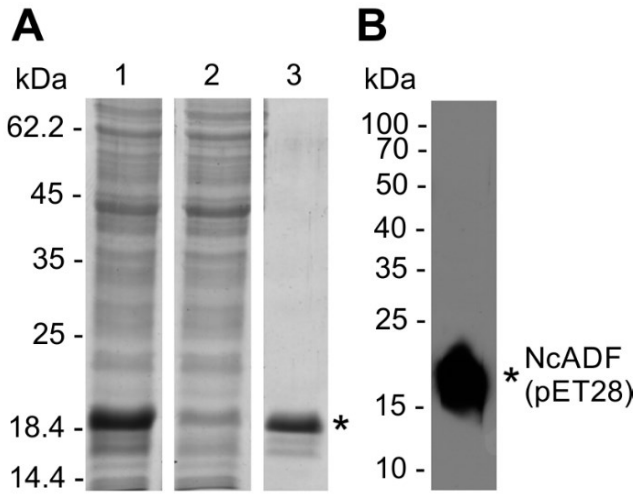

314

Figure 2. Expression of **recombinant NcADF in *E. coli* BL21 (DE3). A)** NcADF was
316 expressed in pET28 after induction with 0.2 mM IPTG growing in TB for 18 hours at room temperature (~22ºC) and purified in Ni^{+2} resin. BL21(DE3) cells were lysed in P buffer (*lane*
318 *1*). NcADF_pET28 was purified and the flow through was collected (*lane 2*). The recombinant protein was eluted and dialysed against the storage buffer (*lane 3*). The gel was stained with
320 Coomassie R-250. **B)** NcADF_pET28 was detected with anti-NcADF serum 1:15,000.

3.3 Interaction with F-actin, but not actin disassembly, is regulated by pH

322 The abilities of NcADF to disassemble actin filaments and interact with F-actin were characterised using a co-sedimentation assay. Both NcADF concentrations (5 and 10 μM) used
324 were able to significantly reduce the amount of actin detected in the pellet as compared with

the actin control without NcADF ($p < 0.05$; *t*-test; 0 μM NcADF vs. 5 μM NcADF and 0 μM NcADF vs. 10 μM NcADF; Figure 3).

The pH-dependence [41] of NcADF activity was analysed using 5 μM F-actin in buffered sedimentation solution, with either a higher or lower pH (8.0 or 6.5, respectively) (Figure 3A and B). The decrease in actin concentration in the pellet was more pronounced in the presence of 10 μM NcADF as compared with 5 μM NcADF, indicating a dose-dependent F-actin disassembly (Figure 3C; $p < 0.05$; *t*-test; 5 μM NcADF vs. 10 μM NcADF). Although present in a two-fold molar excess, NcADF could only disassemble a limited amount of F-actin, with ~75% of total actin remaining in the pellet (Figure 3C). Under neither tested condition was the effect of NcADF on F-actin sedimentation sensitive to pH, demonstrating that pH is not a regulating factor for NcADF activity in F-actin disassembly (Figure 3C; $p > 0.05$; *t*-test; % of actin in the pellet at pH 6.5 vs. pH 8.0). However, the presence of NcADF in the pellet (8.5 ± 0.7%) was observed only at pH 6.5 and with a two-fold molar excess of NcADF (Figure 3B, arrow). The presence of NcADF in the pellet at the lower concentration of pH 6.5 was not observed for two possible reasons: either NcADF did not associate with F-actin at this concentration or the gel staining was not sufficiently sensitive to detect the level of pelleted NcADF (Figure 3B). The possibility of NcADF precipitation at pH 6.5 was ignored due to the absence of NcADF in the control pellet without the addition of actin (Figure 3B). The predicted pI for NcADF is 6.5; however, the 6X-his-tag increased the predicted pI to 8.3, limiting the possibility of precipitation due to pH. Moreover, NcADF was not detected in the pellet at pH 8.0 (Figure 3A). Taken together, these data show that the pH variations did not regulate the activity of NcADF for disassembly of filaments, although the association of NcADF with actin was observed only at pH 6.5, indicating that a stable interaction between NcADF and actin is not required for F-actin disassembly.

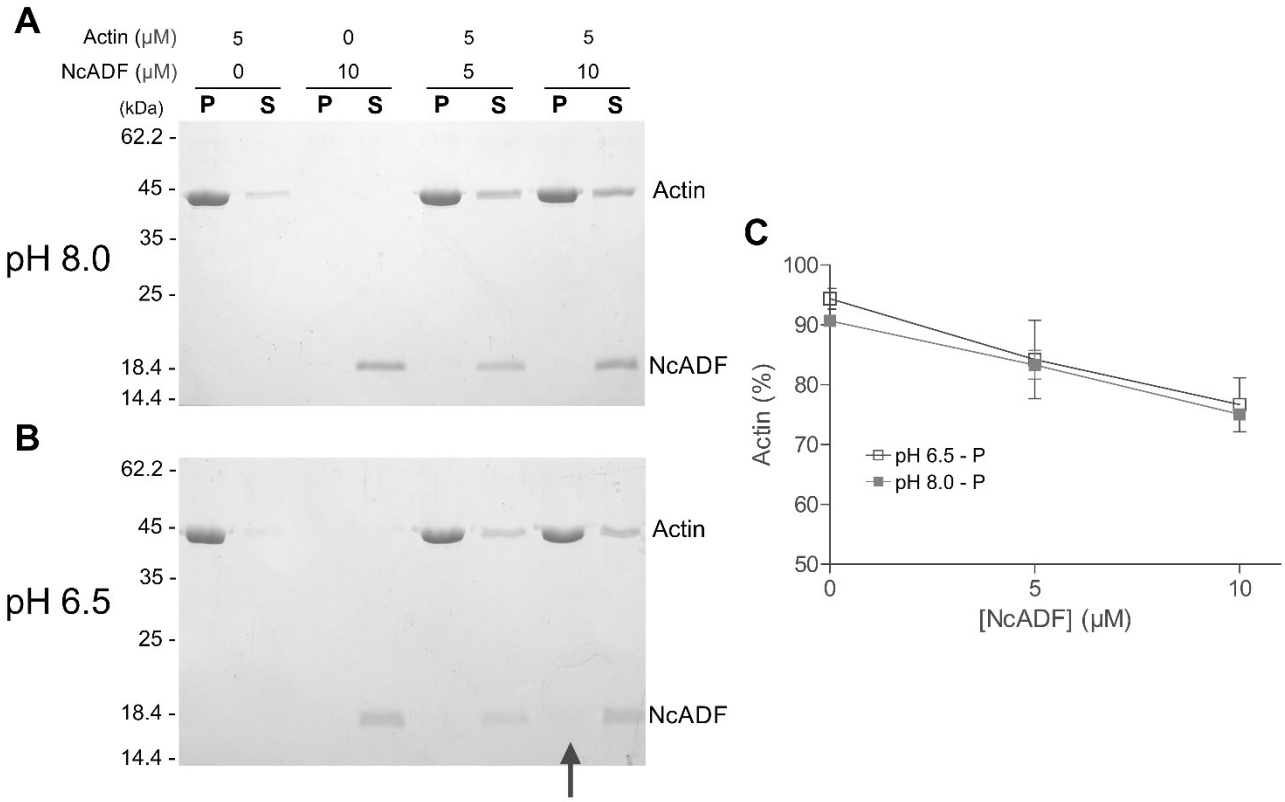

Figure 3. Actin disassembly was analysed in the presence of NcADF in different pH conditions. Rabbit actin (5 μM) was incubated with NcADF (0, 5 or 10 μM) and centrifuged at 105,000 x *g*. Pellet and supernatant were resolved by 12% SDS-PAGE. The gels were stained with Coomassie R-250 and the band densities were quantified. **A)** Representative SDS-PAGE from assay performed at pH 8.0 with pellet (P) and supernatant (S). **B)** Representative gel from assay performed at pH 6.5. The arrow indicates NcADF co-sedimented with F-actin in the pellet. **C)** Effect of pH on the quantity of actin in pellet at pH 6.5 (open black square □) or 8.0 (grey filled square ■) after incubation of 5 μM actin with 5 or 10 μM NcADF. Results were obtained from two independent experiments (mean ± S.E.).

3.4 NcADF increases the polymerisation rate of actin

The effect of NcADF on the kinetics of actin assembly was assessed using PI-actin (10-25%), since the fluorescence of PI-F-actin is approximately 20–25-fold higher than monomeric PI-G-actin [42]. To investigate the effect of NcADF on PI-actin polymerisation, 1, 1.5, 3, or 6 μM NcADF were incubated with PI-actin and the fluorescence was recorded over time. All tested concentrations of NcADF accelerated the initial rate of PI-actin polymerisation (Figure 4A), suggesting a weak severing of filaments by NcADF and the formation of new nuclei for

elongation. When NcADF was present at 6 µM, an overshoot, i.e. a peak in the fluorescence of the polymerised actin followed by a pronounced drop [43], was observed.

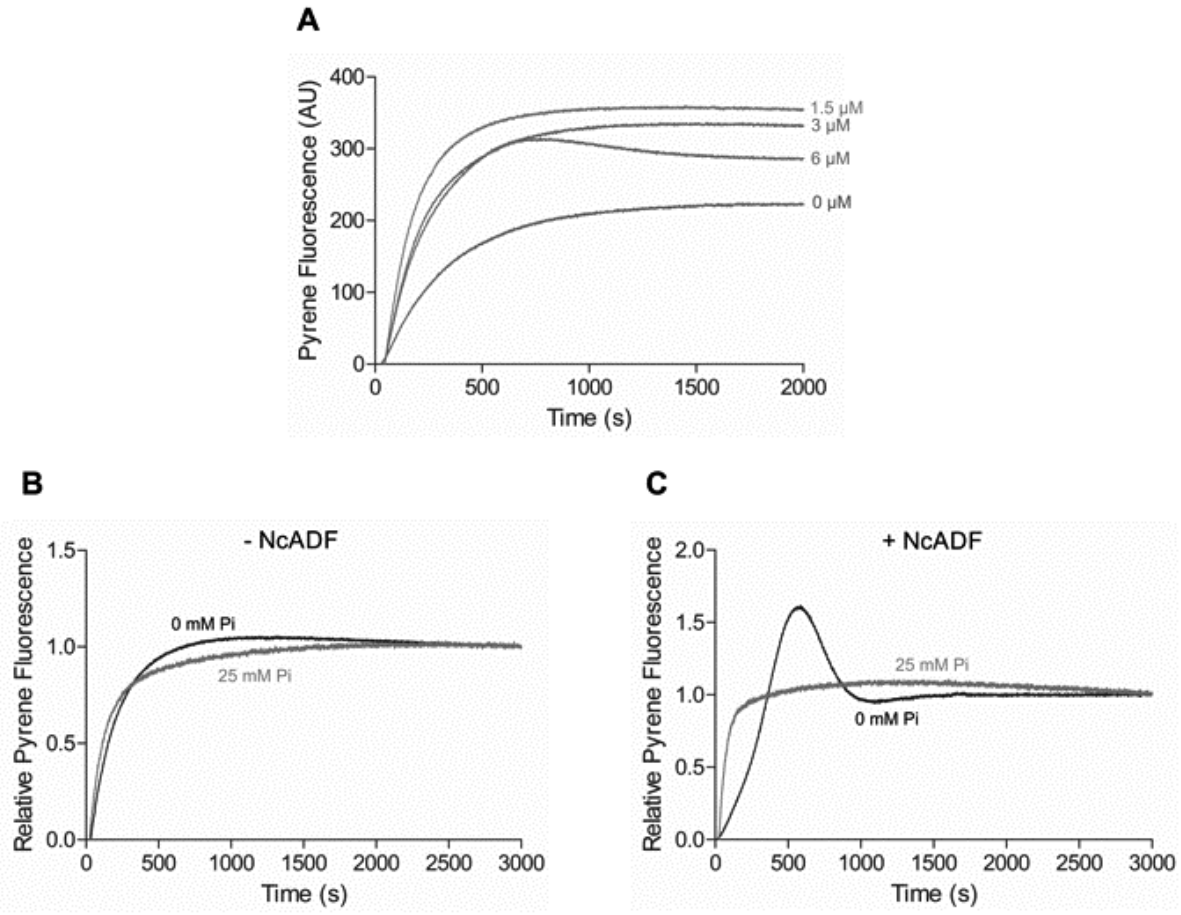

Figure 4. NcADF activity on PI-actin polymerization was investigated. The fluorescence intensity during polymerization of 5 µM rabbit actin (10% PI-actin) was monitored over time (365 nm excitation and 407 nm emission) in the presence of NcADF. **A)** Fluorescence of PI-actin over time after incubation with 0, 1.5, 3 or 6 µM NcADF. **B)** and **C)** PI-actin fluorescence over time with (gray line) or without (black line) 25 mM phosphate buffer (Pi). The data from one experiment were normalised. The experiment was performed without NcADF (- NcADF) **(B)** and with 10 µM NcADF (+ NcADF) **(C)**. Two assays were performed with similar observations.

3.5 Inorganic phosphate inhibits the actin overshoot

To evaluate the effect of inorganic phosphate on PI-actin polymerisation with NcADF, actin was polymerised by the addition of buffer containing 25 mM sodium phosphate pH 8.0. The addition of inorganic phosphate had little effect on PI-actin polymerisation in the control samples (Figure 4B); however, it completely inhibited the overshoot effect of NcADF on the late stage of actin polymerisation (Figure 4B).

3.6 NcADF reduces the fluorescence of PI-F-actin

To investigate the effect of NcADF on PI-F-actin, the fluorescence was measured over time following the addition of various concentrations of NcADF. Initially, the reaction was performed with 1 μM PI-F-actin under ideal polymerisation conditions (50 mM KCl, 2 mM $MgCl_2$, 0.1 mM ATP) and a molar excess of NcADF. The presence of NcADF decreased the fluorescence in a time-dependent manner (Figure 5A). Under these conditions, the control reaction resulted in a relatively small decay in PI-actin fluorescence, and the decrease in fluorescence was dependent on NcADF concentration (Figure 5A). Additionally, NcADF caused a drop in the initial fluorescence, followed by an exponential decay, which was more pronounced at 10 μM NcADF, decreasing the fluorescence to the level of the PI-actin monomer (Figure 5A). As a result of the delay between mixing the proteins and the start of the fluorescence measurement (25 seconds on average), the initial phase was lost. Despite the initial drop, the observed rate constants (kobs) were calculated and plotted against the NcADF concentration, suggesting a non-linear dependence on NcADF concentration (Figure 5A, inset). To avoid the initial drop in fluorescence, the assay was repeated using PI-actin below the critical concentration in low salt buffer, i.e. conditions favouring spontaneous disassembly of filaments, and a lower molar ratio of NcADF and actin. Under these conditions, the initial drop was less pronounced (Figure 5B), indicating that at saturating concentrations, NcADF bound faster to PI-F-actin and quenched the fluorescence. The decay in the initial phase of fluorescence following the addition of 50 and 100 nM NcADF was less pronounced than following the addition of 200 and 400 nM NcADF (Figure 5B). At a 4-fold molar concentration as compared with PI-actin (400 nM), a slow recovery of fluorescence was observed after the initial phase of decay (Figure 5B).

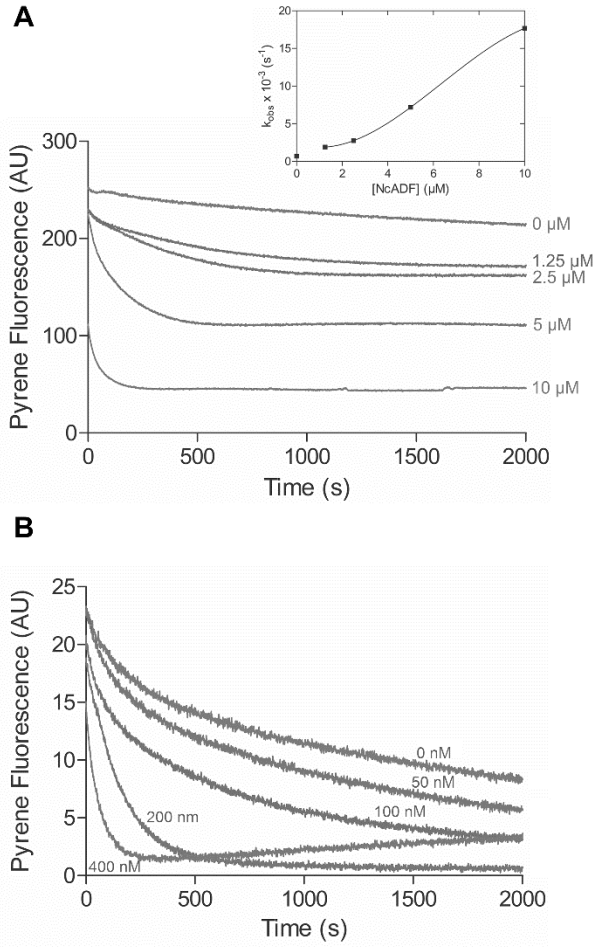

408 **Figure 5. NcADF activity was analysed over PI-F-actin disassembly.** PI-actin filaments were diluted to 1 µM (20% PI-actin) in KMEI (**A**) or 0.1 µM (25% PI-actin) in G-buffer (**B**)
410 and incubated with NcADF. The fluorescence was monitored over time (365 nm excitation and 407 nm emission). **A)** Time course of PI-F-actin fluorescence change upon addition of molar
412 excess of NcADF (0, 1.5, 2.5, 5 and 10 µM). In the inset, dependence of k_{obs} on the concentration of NcADF. The solid line is an illustrative manual fit to the data. **B)** Time course
414 of PI-F-actin fluorescence change upon addition of NcADF (0, 50, 100, 200 and 400 nM NcADF). **A)** and **B)** are the results obtained from a single experiment.

416 **3.7 NcADF reduces the relative viscosity of F-actin**

To investigate the effect of NcADF on the low-shear viscosity of actin, the falling ball assay
418 was employed [44]. The actin polymerisation was induced in mixtures of actin and various concentrations of NcADF. The presence of NcADF reduced the solution's viscosity in a
420 concentration-dependent manner (Figure 6A). At 10 µM, NcADF caused a reduction in viscosity of almost 90% (Figure 6A), evidence that NcADF disassembled actin filaments. The

422 concentrations of gelsolin used in parallel drastically reduced the viscosity and it was not possible to record the time of the falling ball.

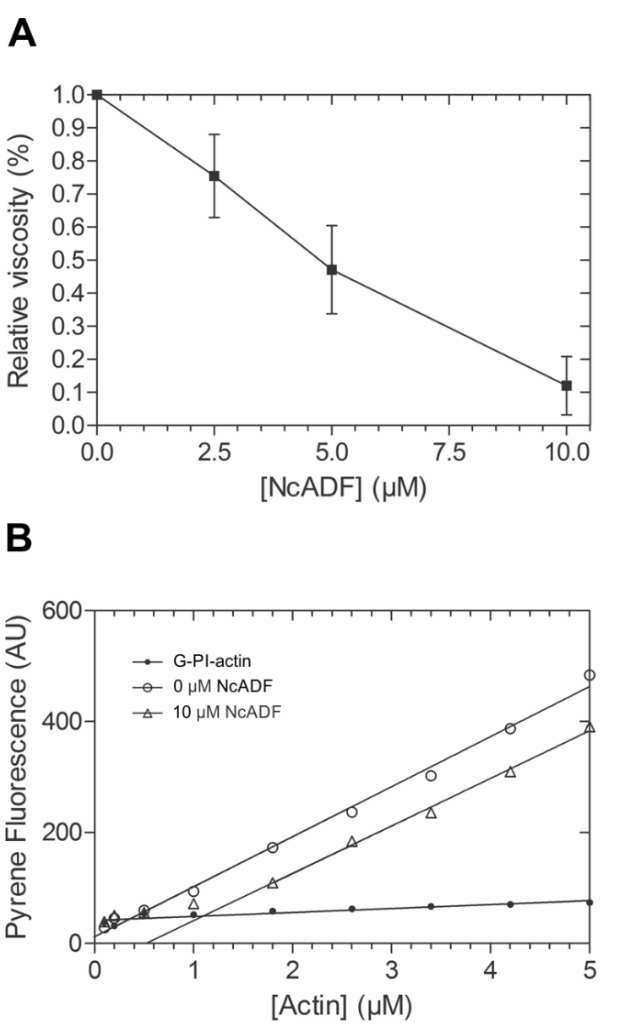

424

Figure 6. Viscosity and critical concentration were analysed in the presence of NcADF.
426 **A)** 10 μM actin was polymerised for 1 h in the presence of 0, 2.5, 5 and 10 μM NcADF by addition of KMET. Viscosity was measured as the velocity of the falling ball. The normalised
428 data shown are resulted from two independent experiments (mean ± SEM). **B)** Actin (10% PI-actin) was serially diluted and aliquots were mixed to either 0 or 10 μM NcADF and the
430 polymerisation was induced by addition of KMEI. After reaching the steady state, the fluorescence was measured. In closed circles (●), non-polymerised PI-actin; in open circles (○), actin
432 polymerised without NcADF; in open triangles (Δ), PI-actin polymerised with 10 μM NaADF. The critical concentration was calculated by the intersection between F-actin with or without
434 NcADF lines and G-actin line. Results from a single experiment.

3.8 NcADF increases the critical concentration of actin

436 To evaluate the effect of NcADF on steady state actin polymerisation, the PI-actin fluorescence was measured following overnight incubation. At 10 μM, NcADF reduced the

438 pyrene signal at steady state at all the concentrations of PI-actin tested above the line of PI-G-actin (Figure 6B). The decrease in PI-actin fluorescence by NcADF at steady state is indicative
440 of monomer sequestration. The critical concentration (Cc) of PI-actin was 0.3 ± 0.083 μM and the Cc of PI-actin in the presence of 10 μM NcADF was 1.1 μM (Figure 6B). The dissociation
442 constant, calculated assuming a 1:1 interaction between NcADF and G-actin, was 4.4 μM. The assay was also performed using lower concentrations of NcADF (1, 2, and 4 μM) mixed with
444 0–4 μM PI-actin. Under these conditions, NcADF reduced the fluorescence and improved the Cc at all the tested concentrations (Figure S3).

446 **3.9 NcADF interacts weakly with ATP-G-actin**

To investigate the binding of NcADF to G-actin, two approaches were used: a protein binding
448 two-dimensional assay and chemical cross-linking by the addition of formaldehyde and EDC. In 2D SDS-PAGE, a vertical coincidence of bands composed of NcADF (Figure 7A, lower
450 molecular mass on arrow) and G-actin (Figure 7A, higher molecular mass on arrow) suggests a weak interaction between the two proteins. Although NcADF and a portion of actin did not
452 completely enter the 1D PAGE gel (Figure 7A, left portion), the trace of NcADF that moved into the 1D PAGE gel was apparently pulled by its binding to actin (Figure 7A, arrows). The
454 smear formed by NcADF at the top of the 1D PAGE gel was observed only when actin was present in the reaction (Figure 7B). A 1D PAGE gel, identical the one used over the 2D SDS-
456 PAGE, was stained and three bands were visualised; a band with higher mobility, an intermediate band, and a band that moved slowly. The same stained gel is shown horizontally
458 over the SDS gel (Figure 7A) and vertically in Figure 7B. The coincidence of proteins in the 2D SDS-PAGE gel was compatible with the intermediate band formed in the 1D PAGE gel
460 (Figure 7A and B, asterisk). NcADF on top of the gel and in the intermediate band was detected by the anti-NcADF serum (Figure 7B), confirming the presence of NcADF.

462 Two chemical cross-linking agents were used to visualise the binding of NcADF to G-actin. Initially, 4% formaldehyde was added to the interaction buffer with NcADF in the presence of
464 G-actin. A band of 60 kDa was formed (Figure 7C, arrow and asterisk), corresponding to the sum of the molecular masses of NcADF (18 kDa) and actin (42 kDa). NcADF was detected by
466 the anti-NcADF serum in the two bands of 18 kDa (Figure 7D) and 60 kDa (Figure 7D, arrow), strongly indicative of NcADF binding to G-actin. The presence of a band at 60 kDa was also
468 observed when formaldehyde was replaced with EDC and the gel was stained (Figure 7E).

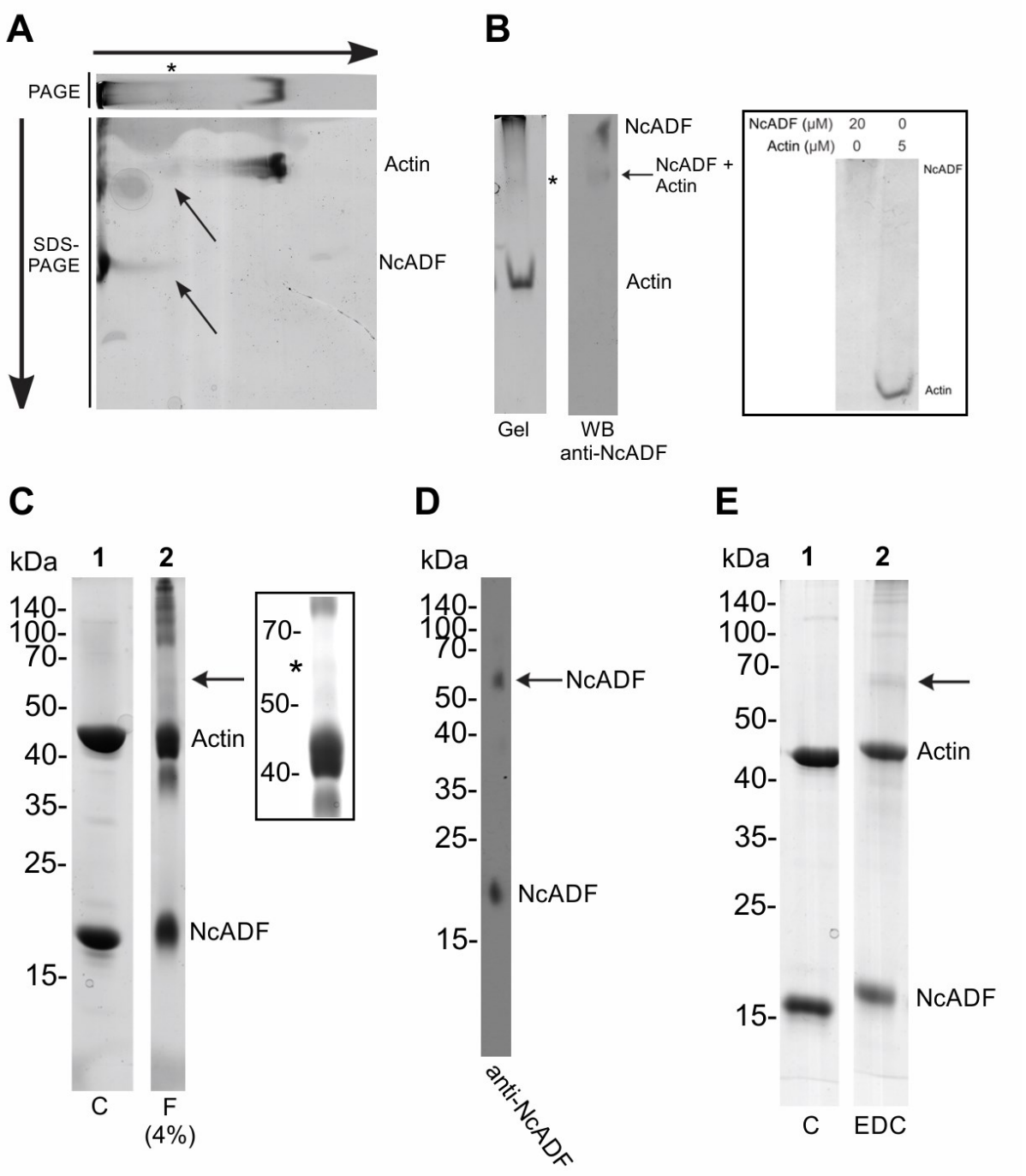

470 **Figure 7. The ability of NcADF to bind to rabbit G-actin was evaluated. A)** Two-
dimensional electrophoresis using actin (5 μM) and NcADF (20μM). Horizontally, a 7,5%
472 PAGE strip containing the reaction. Above the strip, the 12.5% SDS-PAGE. The larger arrows
indicate the direction of the run and the smaller arrows show the region where NcADF and
474 actin overlap in PAGE. **B)** The same PAGE gel strip shown in **A** and respective western
blotting detection of NcADF with anti-NcADF serum (1:15,000). In the asterisk (*), the band
476 containing NcADF and actin. In the inset inside rectangle, the control reaction, containing
either actin or NcADF. **C)** 12.5% SDS-PAGE. Mixture of actin (10 μM) and NcADF (10 μM)
478 incubated with (*lane 2*) or without (*lane 1*) 4% formaldehyde. C = control; F = formaldehyde.
In arrow, the 60-kDa band. In the inset inside rectangle, a zoomed image of lane 2 with bright
480 and contrast adjusted to visualise the 60-kDa band (in asterisk). **D)** Western blotting using the

same reaction shown in C, *lane 2*. NcADF was detected by anti-NcADF serum (1:10,000). The
482 arrow, NcADF detected with 60-kDa. **E)** 12.5% SDS-PAGE. Actin (5 µM) was incubated with NcADF (5 µM) with (*lane 2*) or without (*lane 1*) 2 mM EDC. C = control. The arrow indicates
484 the 60-kDa band.

4. Discussion

486 Here, we studied *N. caninum* actin-depolymerisation factor (NcADF), a ubiquitous protein that belongs to the ADF/cofilin family and is important for regulation of actin functions in
488 eukaryotes [45]. To investigate the role of NcADF in actin dynamics, we used a recombinant N-terminally 6X-his-tagged NcADF and rabbit skeletal actin. Mammalian skeletal muscle
490 actin has been widely employed for the investigation of ADF/cofilins from different species [46-50], including apicomplexan ADFs [23, 26, 27] due to its use in well-established protocols
492 and its convenience. These studies allow the potential comparative analysis of ADF/cofilin functions among species. Computational analysis was performed in parallel to biochemical
494 approaches to give structural and functional insight into NcADF. Important residues for actin binding have been identified in yeast cofilin by site-specific mutagenesis [51] and synchrotron
496 protein footprinting [52]. The amino acids identified in yeast cofilin responsible for G-actin binding are conserved among the ADF/cofilins; however, crucial differences were found in
498 NcADF when F-actin binding sites were considered. The F-loop, located between β-4 and β-5 and typically protruding out of the structure in canonical ADF/cofilins, is shorter in NcADF,
500 consistent with observations of other apicomplexan ADFs [24, 25]. Additionally, the C-terminal charged residues, identified to be important for F-actin binding, which is usually
502 folded in an α-4 helix in other ADF/cofilins, are truncated in NcADF and other apicomplexan ADFs [26, 53], with the exception of PfADF2 [24]. In NcADF, these differences within the F-
504 actin binding sites were expected given the similarity to TgADF; however, the C-terminal α-4 helix, present in PfADF1 and predicted to be one turn in NcADF, is absent in TgADF. The
506 G112 in TgADF (which corresponds to S112 in NcADF and Q115 in PfADF1) may be responsible for the absence of the α-4 helix, due to the low propensity of glycine to form α-

508 helices [54]. In the alignment (Figure 1), S112 in NcADF corresponds to E126 in yeast cofilin, which has been identified as a G-actin binding site [6]. However, there is no evidence that these
510 residues are involved in the functional differences among these proteins.

Despite the absence of canonical F-actin binding sites, NcADF bound stably to F-actin. The
512 relatively low binding affinity of NcADF for F-actin was observed in a co-sedimentation assay only at pH 6.5. Certain ADF/cofilins, especially from higher vertebrates, exhibit pH-dependent
514 activity, regulating F-actin binding and F-actin disassembly [18]. In coccidians, pH may regulate only F-actin binding to ADFs as observed with NcADF and TgADF [23]. PfADF1, in
516 contrast, did not co-sediment with actin by ultracentrifugation at either pH 6.5 or 8.5 [27]. The ability to disassemble actin filaments was not changed upon pH variation with NcADF,
518 TgADF, or PfADF1 [23, 27]. The pH-dependence only for stable F-actin binding, but not for F-actin disassembly may be a consequence of a mechanism other than severing or
520 depolymerisation, indicating monomer sequestration as observed in *C. elegans* (UNC60A) [55], depactin from starfish oocysts [56], and TgADF [23]. The ability of NcADF to
522 disassemble filaments was weak as compared with TgADF [23]. In a 1:1 molar ratio with actin, NcADF caused a smaller decrease in actin in the pellet as compared with TgADF [23]. The
524 high sequence identity between the two coccidian ADFs may not be indicative of an identical function and requires a specific investigation of non-conserved regions to determine eventual
526 functional differences. Other possibilities are either an influence of the ADF's N-terminal his-tag on the interaction with actin or variations in co-sedimentation protocols and gel staining
528 used in both studies. The cleavage of the tag would have avoided a possible ambiguity in the interpretation of data. However, several studies used His-tagged ADF/cofilins which
530 apparently did not affect the activity of protein [20, 23, 46, 49].

Affinity of NcADF for F-actin, as assessed by a co-sedimentation assay, was also observed
532 as the quenching of PI-actin fluorescence. The pyrene fluorescence is higher when the

fluorophore is associated with filaments as compared with monomers [42], but the signal is not linearly proportional to the incorporation of monomers into filaments [57]. The interaction of ADF/cofilins and PI-F-actin has been determined to quench the pyrene fluorescence [58-60]. Moreover, the quenching may be a consequence of different mechanisms such as binding, depolymerisation, or conformational changes [58]. Additionally, this decrease in pyrene fluorescence has been previously used to measure the binding of a molar excess of actophorin to F-actin [58]. Under filament-stabilisation conditions and a molar excess of NcADF, a drop in the initial fluorescence as compared with the control without NcADF is indicative of filament binding. It is likely that the subsequent exponential decline is the consequence of PI-F-actin binding to NcADF associated with disassembly. The non-linearity of the plot of observed rate constants versus NcADF concentrations may reflect different mechanisms of action. The use of actin depolymerisation conditions and a lower molar ratio of NcADF and PI-F-actin still showed an initial drop in fluorescence, indicating binding and/or filament disassembly. Despite the challenging data interpretation due to the quenching of the pyrene fluorescence, the NcADF concentration-dependent reduction in low-shear viscosity of the F-actin solution confirms that actin net filament was disassembled. The reduction in viscosity is strong evidence for a decrease in the extent of net filament and has previously been associated with filament severing [38, 47]. Relative to actophorin and human ADF (HsADF), NcADF has a weak effect on actin filaments, since 10 μM NcADF was necessary to reduce the viscosity by the same amount as 1 μM actophorin and 8 μM human ADF [47]. The weak actin disassembly by NcADF observed by viscometry is consistent with co-sedimentation findings.

In the polymerisation kinetics assay, NcADF may sever the generated filaments, stimulating PI-actin polymerisation under all conditions. Similar observations were obtained with actophorin [61], *Arabidopsis thaliana* ADF1[59], and cofilin [60]. Other apicomplexan ADFs exhibit different effects on actin polymerisation kinetics. TgADF improves the polymerisation

558 rate at lower concentrations and inhibits mammal actin nucleation and polymerisation at two-
fold molar excess [23]. PfADF1 has no effect on actin polymerisation [24, 27], while PfADF2
560 inhibits polymerisation at a 1:1 molar ratio with actin [27]. At higher concentrations, NcADF
caused the known effect of ADF/cofilins on the polymerisation curve; the overshoot. This
562 effect is not likely to be an artefact of pyrene fluorescence [43] and has been attributed to the
severing of F-actin by homologous ADF/cofilins [38, 55, 60, 62, 63]. The overshoot was
564 completely inhibited in the presence of inorganic phosphate (Pi). It has been previously shown
that Pi is antagonistic of ADF/cofilins in the binding of F-actin [58, 64] by cooperative binding
566 of Pi to actin [64]. Thus, the inhibition of the overshoot by Pi may be a result of the inhibition
of NcADF binding to F-actin, preventing filament severing. This mechanism is suggestive of
568 ADF/cofilin activity regulation by Pi in cells.

Certain ADF/cofilins can interfere with the steady state of actin, when the dissociation and
570 association rates of the monomers at both ends of the actin filament are balanced, enhancing
actin turnover [65]. NcADF increased the critical concentration of actin at steady state and
572 reduced the PI-F-actin fluorescence, indicating inhibition of actin polymerisation and the
binding to monomers. Typical monomer sequestering substances and proteins such as
574 latrunculin A [66] and β-tymosins [59, 67], respectively, show similar results. Actophorin,
HsADF, and *A. thaliana* ADF1 (AtADF1) are ADF/cofilin homologous that inhibit
576 polymerisation and reduce actin critical concentration [27, 38, 41]. Unlike PfADF1, which does
not affect the fluorescence of PI-actin at steady state [27], TgADF inhibits actin polymerisation
578 at a 2.5-fold molar excess [23]. Another explanation for the observed decrease in fluorescence
is that NcADF may bind to PI-F-actin and quench the fluorescence.

580 The PAGE and chemical cross-linking assays demonstrated a low affinity of NcADF for G-
actin. The band formed by the NcADF-G-actin complex has been observed in previous cross-
582 linking assays [25, 38, 68, 69], being compatible with the sum of their molecular weights. The

use of formaldehyde as a cross-linker also confirmed the presence of an NcADF-G-actin complex. NcADF was detected in two bands (18 kDa and the 60-kDa complex), even though formaldehyde may interfere with protein migration and western blotting transfer efficiency. The anti-NcADF serum also detected the endogenous protein in cell extract of *N. caninum* by western blot and extracellular tachyzoites by immunofluorescence (not shown; to be published elsewhere).

Collectively, the present results show that the 6X his-tagged NcADF displays a relatively weak activity in the disassembly of rabbit muscle F-actin, which is not regulated by pH. The low affinity for F-actin indicates that actin disassembly may occur by transient interaction of NcADF and F-actin via a yet undescribed mechanism. In addition, the low affinity between NcADF and G-actin suggests that, although present, monomer sequestration is not the main mechanism of F-actin disassembly by NcADF under the tested conditions. The F-actin disassembly may be primarily caused by severing. The characterisation of NcADF extends our understanding of ADF/cofilin conservation and their function across the phylum *Apicomplexa*. Furthermore, it represents a contribution towards the understanding of actin dynamics modulation, and in the future, may provide information regarding important mechanisms of dissemination and survival of the parasite in its wide range of hosts.

5. Funding

This work was supported by Fundação de Amparo à Pesquisa do Estado de São Paulo (FAPESP) (grant numbers 2012/22772-2 and 2015/04258-8).

6. Acknowledgments

We would like to thank Maraísa Palhão Verri for the technical support in mice immunisation. LB would like to acknowledge all SKM lab members for the lab accession and assistance.

7. References

[1] J. Dubey, G. Schares, Neosporosis in animals-The last five years, Veterinary Parasitology 180(1-2) (2011) 90-108.
[2] M. Reichel, M. Ayanegui-Alcerreca, L. Gondim, J. Ellis, What is the global economic impact of Neospora caninum in cattle - The billion dollar question, International Journal For Parasitology 43(2) (2013) 133-142.
[3] I. Tardieux, J. Baum, Reassessing the mechanics of parasite motility and host-cell invasion, J Cell Biol 214(5) (2016) 507-15.
[4] J. Baum, A.T. Papenfuss, B. Baum, T.P. Speed, A.F. Cowman, Regulation of apicomplexan actin-based motility, Nat Rev Microbiol 4(8) (2006) 621-8.
[5] J.M. Dobrowolski, L.D. Sibley, Toxoplasma invasion of mammalian cells is powered by the actin cytoskeleton of the parasite, Cell 84(6) (1996) 933-9.
[6] D.M. Wetzel, S. Håkansson, K. Hu, D. Roos, L.D. Sibley, Actin filament polymerization regulates gliding motility by apicomplexan parasites, Mol Biol Cell 14(2) (2003) 396-406.
[7] N. Andenmatten, S. Egarter, A.J. Jackson, N. Jullien, J.P. Herman, M. Meissner, Conditional genome engineering in Toxoplasma gondii uncovers alternative invasion mechanisms, Nat Methods 10(2) (2013) 125-7.
[8] S. Egarter, N. Andenmatten, A.J. Jackson, J.A. Whitelaw, G. Pall, J.A. Black, D.J. Ferguson, I. Tardieux, A. Mogilner, M. Meissner, The toxoplasma Acto-MyoA motor complex is important but not essential for gliding motility and host cell invasion, PLoS One 9(3) (2014) e91819.
[9] J.A. Whitelaw, F. Latorre-Barragan, S. Gras, G.S. Pall, J.M. Leung, A. Heaslip, S. Egarter, N. Andenmatten, S.R. Nelson, D.M. Warshaw, G.E. Ward, M. Meissner, Surface attachment, promoted by the actomyosin system of Toxoplasma gondii is important for efficient gliding motility and invasion, BMC Biol 15(1) (2017) 1.
[10] N. Sahoo, W. Beatty, J. Heuser, D. Sept, L. Sibley, Unusual kinetic and structural properties control rapid assembly and turnover of actin in the parasite Toxoplasma gondii, Molecular Biology of the Cell 17(2) (2006) 895-906.
[11] S. Schmitz, M. Grainger, S. Howell, L.J. Calder, M. Gaeb, J.C. Pinder, A.A. Holder, C. Veigel, Malaria parasite actin filaments are very short, J Mol Biol 349(1) (2005) 113-25.
[12] K.M. Skillman, C.I. Ma, D.H. Fremont, K. Diraviyam, J.A. Cooper, D. Sept, L.D. Sibley, The unusual dynamics of parasite actin result from isodesmic polymerization, Nat Commun 4 (2013) 2285.
[13] E.P. Kumpula, I. Pires, D. Lasiwa, H. Piirainen, U. Bergmann, J. Vahokoski, I. Kursula, Apicomplexan actin polymerization depends on nucleation, Sci Rep 7(1) (2017) 12137.
[14] H. Schüler, K. Matuschewski, Regulation of apicomplexan microfilament dynamics by a minimal set of actin-binding proteins, Traffic 7(11) (2006) 1433-9.
[15] S.K. Maciver, P.J. Hussey, The ADF/cofilin family: actin-remodeling proteins, Genome Biol 3(5) (2002) reviews3007.
[16] M. Poukkula, E. Kremneva, M. Serlachius, P. Lappalainen, Actin-depolymerizing factor homology domain: a conserved fold performing diverse roles in cytoskeletal dynamics, Cytoskeleton (Hoboken) 68(9) (2011) 471-90.
[17] G. Kanellos, M.C. Frame, Cellular functions of the ADF/cofilin family at a glance, J Cell Sci 129(17) (2016) 3211-8.
[18] G. Hild, L. Kalmár, R. Kardos, M. Nyitrai, B. Bugyi, The other side of the coin: functional and structural versatility of ADF/cofilins, Eur J Cell Biol 93(5-6) (2014) 238-51.
[19] E. Andrianantoandro, T.D. Pollard, Mechanism of actin filament turnover by severing and nucleation at different concentrations of ADF/cofilin, Mol Cell 24(1) (2006) 13-23.
[20] M.L. Allen, J.M. Dobrowolski, H. Muller, L.D. Sibley, T.E. Mansour, Cloning and characterization of actin depolymerizing factor from Toxoplasma gondii, Mol Biochem Parasitol 88(1-2) (1997) 43-52.

[21] S. Haase, D. Zimmermann, M.A. Olshina, M. Wilkinson, F. Fisher, Y.H. Tan, R.J. Stewart, C.J. Tonkin, W. Wong, D.R. Kovar, J. Baum, Disassembly activity of actin-depolymerizing factor (ADF) is associated with distinct cellular processes in apicomplexan parasites, Mol Biol Cell 26(17) (2015) 3001-12.
[22] S. Mehta, L.D. Sibley, Actin depolymerizing factor controls actin turnover and gliding motility in Toxoplasma gondii, Mol Biol Cell 22(8) (2011) 1290-9.
[23] S. Mehta, L.D. Sibley, Toxoplasma gondii actin depolymerizing factor acts primarily to sequester G-actin, J Biol Chem 285(9) (2010) 6835-47.
[24] B.K. Singh, J.M. Sattler, M. Chatterjee, J. Huttu, H. Schüler, I. Kursula, Crystal structures explain functional differences in the two actin depolymerization factors of the malaria parasite, J Biol Chem 286(32) (2011) 28256-64.
[25] W. Wong, A.I. Webb, M.A. Olshina, G. Infusini, Y.H. Tan, E. Hanssen, B. Catimel, C. Suarez, M. Condron, F. Angrisano, T. Nebi, D.R. Kovar, J. Baum, A mechanism for actin filament severing by malaria parasite actin depolymerizing factor 1 via a low affinity binding interface, J Biol Chem 289(7) (2014) 4043-54.
[26] W. Wong, C.T. Skau, D.S. Marapana, E. Hanssen, N.L. Taylor, D.T. Riglar, E.S. Zuccala, F. Angrisano, H. Lewis, B. Catimel, O.B. Clarke, N.J. Kershaw, M.A. Perugini, D.R. Kovar, J.M. Gulbis, J. Baum, Minimal requirements for actin filament disassembly revealed by structural analysis of malaria parasite actin-depolymerizing factor 1, Proc Natl Acad Sci U S A 108(24) (2011) 9869-74.
[27] H. Schüler, A.K. Mueller, K. Matuschewski, A Plasmodium actin-depolymerizing factor that binds exclusively to actin monomers, Mol Biol Cell 16(9) (2005) 4013-23.
[28] Y. Doi, N. Shinzawa, S. Fukumoto, H. Okano, H. Kanuka, ADF2 is required for transformation of the ookinete and sporozoite in malaria parasite development, Biochem Biophys Res Commun 397(4) (2010) 668-72.
[29] B. Gajria, A. Bahl, J. Brestelli, J. Dommer, S. Fischer, X. Gao, M. Heiges, J. Iodice, J.C. Kissinger, A.J. Mackey, D.F. Pinney, D.S. Roos, C.J. Stoeckert, H. Wang, B.P. Brunk, ToxoDB: an integrated Toxoplasma gondii database resource, Nucleic Acids Res 36(Database issue) (2008) D553-6.
[30] M. Punta, P.C. Coggill, R.Y. Eberhardt, J. Mistry, J. Tate, C. Boursnell, N. Pang, K. Forslund, G. Ceric, J. Clements, A. Heger, L. Holm, E.L. Sonnhammer, S.R. Eddy, A. Bateman, R.D. Finn, The Pfam protein families database, Nucleic Acids Res 40(Database issue) (2012) D290-301.
[31] K.B. Nicholas, GeneDoc: analysis and visualization of genetic variation.
[32] N. Eswar, D. Eramian, B. Webb, M.Y. Shen, A. Sali, Protein structure modeling with MODELLER, Methods Mol Biol 426 (2008) 145-59.
[33] D. Xu, Y. Zhang, Improving the physical realism and structural accuracy of protein models by a two-step atomic-level energy minimization, Biophys J 101(10) (2011) 2525-34.
[34] R.A. Laskowski, M.W. MacArthur, J.A. Thornton, PROCHECK: a program to check the stereochemical quality of protein structures., Journal of Applied Crystallography 26 (1993) 283-291.
[35] D. Eisenberg, R. Lüthy, J.U. Bowie, VERIFY3D: assessment of protein models with three-dimensional profiles, Methods Enzymol 277 (1997) 396-404.
[36] V.B. Chen, W.B. Arendall, J.J. Headd, D.A. Keedy, R.M. Immormino, G.J. Kapral, L.W. Murray, J.S. Richardson, D.C. Richardson, MolProbity: all-atom structure validation for macromolecular crystallography, Acta Crystallogr D Biol Crystallogr 66(Pt 1) (2010) 12-21.
[37] L.M. Pereira, J.A. Candido-Silva, E. De Vries, A.P. Yatsuda, A new thrombospondin-related anonymous protein homologue in Neospora caninum (NcMIC2-like1), Parasitology 138(3) (2011) 287-97.

706 [38] S.K. Maciver, H.G. Zot, T.D. Pollard, Characterization of actin filament severing by actophorin from Acanthamoeba castellanii, J Cell Biol 115(6) (1991) 1611-20.
708 [39] M.F. Carlier, C. Jean, K.J. Rieger, M. Lenfant, D. Pantaloni, Modulation of the interaction between G-actin and thymosin beta 4 by the ATP/ADP ratio: possible implication in the
710 regulation of actin dynamics, Proc Natl Acad Sci U S A 90(11) (1993) 5034-8.
[40] R. Gurung, R. Yadav, J.G. Brungardt, A. Orlova, E.H. Egelman, M.R. Beck, Actin
712 polymerization is stimulated by actin cross-linking protein palladin, Biochem J 473(4) (2016) 383-96.
714 [41] M. Hawkins, B. Pope, S.K. Maciver, A.G. Weeds, Human actin depolymerizing factor mediates a pH-sensitive destruction of actin filaments, Biochemistry 32(38) (1993) 9985-93.
716 [42] T. Kouyama, K. Mihashi, Fluorimetry study of N-(1-pyrenyl)iodoacetamide-labelled F-actin. Local structural change of actin protomer both on polymerization and on binding of
718 heavy meromyosin, Eur J Biochem 114(1) (1981) 33-8.
[43] F.J. Brooks, A.E. Carlsson, Actin polymerization overshoots and ATP hydrolysis as
720 assayed by pyrene fluorescence, Biophys J 95(3) (2008) 1050-62.
[44] S.D. MacLean-Fletcher, T.D. Pollard, Viscometric analysis of the gelation of
722 Acanthamoeba extracts and purification of two gelation factors, J Cell Biol 85(2) (1980) 414-28.
724 [45] P. Lappalainen, M.M. Kessels, M.J. Cope, D.G. Drubin, The ADF homology (ADF-H) domain: a highly exploited actin-binding module, Mol Biol Cell 9(8) (1998) 1951-9.
726 [46] K. Dai, S. Liao, J. Zhang, X. Zhang, X. Tu, Structural and functional insight into ADF/cofilin from Trypanosoma brucei, PLoS One 8(1) (2013) e53639.
728 [47] S.K. Maciver, B.J. Pope, S. Whytock, A.G. Weeds, The effect of two actin depolymerizing factors (ADF/cofilins) on actin filament turnover: pH sensitivity of F-actin binding by human
730 ADF, but not of Acanthamoeba actophorin, Eur J Biochem 256(2) (1998) 388-97.
[48] F. Ressad, D. Didry, G.X. Xia, Y. Hong, N.H. Chua, D. Pantaloni, M.F. Carlier, Kinetic
732 analysis of the interaction of actin-depolymerizing factor (ADF)/cofilin with G- and F-actins. Comparison of plant and human ADFs and effect of phosphorylation, J Biol Chem 273(33)
734 (1998) 20894-902.
[49] T.V. Tammana, A.A. Sahasrabuddhe, K. Mitra, V.K. Bajpai, C.M. Gupta, Actin-
736 depolymerizing factor, ADF/cofilin, is essentially required in assembly of Leishmania flagellum, Mol Microbiol 70(4) (2008) 837-52.
738 [50] S. Yamashiro, K. Mohri, S. Ono, The two Caenorhabditis elegans actin-depolymerizing factor/cofilin proteins differently enhance actin filament severing and depolymerization,
740 Biochemistry 44(43) (2005) 14238-47.
[51] P. Lappalainen, E.V. Fedorov, A.A. Fedorov, S.C. Almo, D.G. Drubin, Essential functions
742 and actin-binding surfaces of yeast cofilin revealed by systematic mutagenesis, EMBO J 16(18) (1997) 5520-30.
744 [52] J.Q. Guan, S. Vorobiev, S.C. Almo, M.R. Chance, Mapping the G-actin binding surface of cofilin using synchrotron protein footprinting, Biochemistry 41(18) (2002) 5765-75.
746 [53] R. Yadav, P.P. Pathak, V.K. Shukla, A. Jain, S. Srivastava, S. Tripathi, S.V. Krishna Pulavarti, S. Mehta, L.D. Sibley, A. Arora, Solution structure and dynamics of ADF from
748 Toxoplasma gondii, J Struct Biol 176(1) (2011) 97-111.
[54] J.W. Bryson, S.F. Betz, H.S. Lu, D.J. Suich, H.X. Zhou, K.T. O'Neil, W.F. DeGrado,
750 Protein design: a hierarchic approach, Science 270(5238) (1995) 935-41.
[55] S. Ono, G.M. Benian, Two Caenorhabditis elegans actin depolymerizing factor/cofilin
752 proteins, encoded by the unc-60 gene, differentially regulate actin filament dynamics, J Biol Chem 273(6) (1998) 3778-83.
754 [56] I. Mabuchi, An actin-depolymerizing protein (depactin) from starfish oocytes: properties and interaction with actin, J Cell Biol 97(5 Pt 1) (1983) 1612-21.

[57] E. Grazi, Polymerization of N-(1-pyrenyl) iodoacetamide-labelled actin: the fluorescence signal is not directly proportional to the incorporation of the monomer into the polymer, Biochem Biophys Res Commun 128(3) (1985) 1058-63.

[58] L. Blanchoin, T.D. Pollard, Mechanism of interaction of Acanthamoeba actophorin (ADF/Cofilin) with actin filaments, J Biol Chem 274(22) (1999) 15538-46.

[59] M.F. Carlier, V. Laurent, J. Santolini, R. Melki, D. Didry, G.X. Xia, Y. Hong, N.H. Chua, D. Pantaloni, Actin depolymerizing factor (ADF/cofilin) enhances the rate of filament turnover: implication in actin-based motility, J Cell Biol 136(6) (1997) 1307-22.

[60] A.L. Moon, P.A. Janmey, K.A. Louie, D.G. Drubin, Cofilin is an essential component of the yeast cortical cytoskeleton, J Cell Biol 120(2) (1993) 421-35.

[61] S.K. Maciver, A.G. Weeds, Actophorin preferentially binds monomeric ADP-actin over ATP-bound actin: consequences for cell locomotion, FEBS Lett 347(2-3) (1994) 251-6.

[62] J.A. Cooper, J.D. Blum, R.C. Williams, T.D. Pollard, Purification and characterization of actophorin, a new 15,000-dalton actin-binding protein from Acanthamoeba castellanii, J Biol Chem 261(1) (1986) 477-85.

[63] J. Du, C. Frieden, Kinetic studies on the effect of yeast cofilin on yeast actin polymerization, Biochemistry 37(38) (1998) 13276-84.

[64] A. Muhlrad, D. Pavlov, Y.M. Peyser, E. Reisler, Inorganic phosphate regulates the binding of cofilin to actin filaments, FEBS J 273(7) (2006) 1488-96.

[65] J.A. Theriot, Accelerating on a treadmill: ADF/cofilin promotes rapid actin filament turnover in the dynamic cytoskeleton, J Cell Biol 136(6) (1997) 1165-8.

[66] M. Coué, S.L. Brenner, I. Spector, E.D. Korn, Inhibition of actin polymerization by latrunculin A, FEBS Lett 213(2) (1987) 316-8.

[67] F.X. Yu, S.C. Lin, M. Morrison-Bogorad, M.A. Atkinson, H.L. Yin, Thymosin beta 10 and thymosin beta 4 are both actin monomer sequestering proteins, J Biol Chem 268(1) (1993) 502-9.

[68] R.A. Gungabissoon, C.-J. Jiang, B.K. Drøbak, S.K. Maciver, P.J. Hussey, Interaction of maize actin-depolymerising factor with actin and phosphoinositides and its inhibition of plant phospholipase C, 16(6) (1998) 689-696.

[69] H.G. Mannherz, E. Ballweber, M. Galla, S. Villard, C. Granier, C. Steegborn, A. Schmidtmann, K. Jaquet, B. Pope, A.G. Weeds, Mapping the ADF/cofilin binding site on monomeric actin by competitive cross-linking and peptide array: evidence for a second binding site on monomeric actin, J Mol Biol 366(3) (2007) 745-55.